

2022-06-01

Sources, concentrations, distributions, fluxes and fate of microplastics in a hypersaline lake: Maharloo, south-west Iran

Abbasi, S

<http://hdl.handle.net/10026.1/19184>

10.1016/j.scitotenv.2022.153721

Science of the Total Environment

Elsevier

All content in PEARL is protected by copyright law. Author manuscripts are made available in accordance with publisher policies. Please cite only the published version using the details provided on the item record or document. In the absence of an open licence (e.g. Creative Commons), permissions for further reuse of content should be sought from the publisher or author.

1 **Sources, concentrations, distributions, fluxes and fate of microplastics in a**
2 **hypersaline lake: Maharloo, south-west Iran**

3
4 Sajjad Abbasi ^{a,b*}, Andrew Turner ^c

5
6 ^a Department of Earth Sciences, College of Science, Shiraz University, Shiraz, 71454, Iran

7 ^b Department of Radiochemistry and Environmental Chemistry, Faculty of Chemistry, Maria Curie-
8 Skłodowska University, Lublin 20-031, Poland

9 ^c School of Geography, Earth and Environmental Sciences, University of Plymouth, PL4 8AA, UK

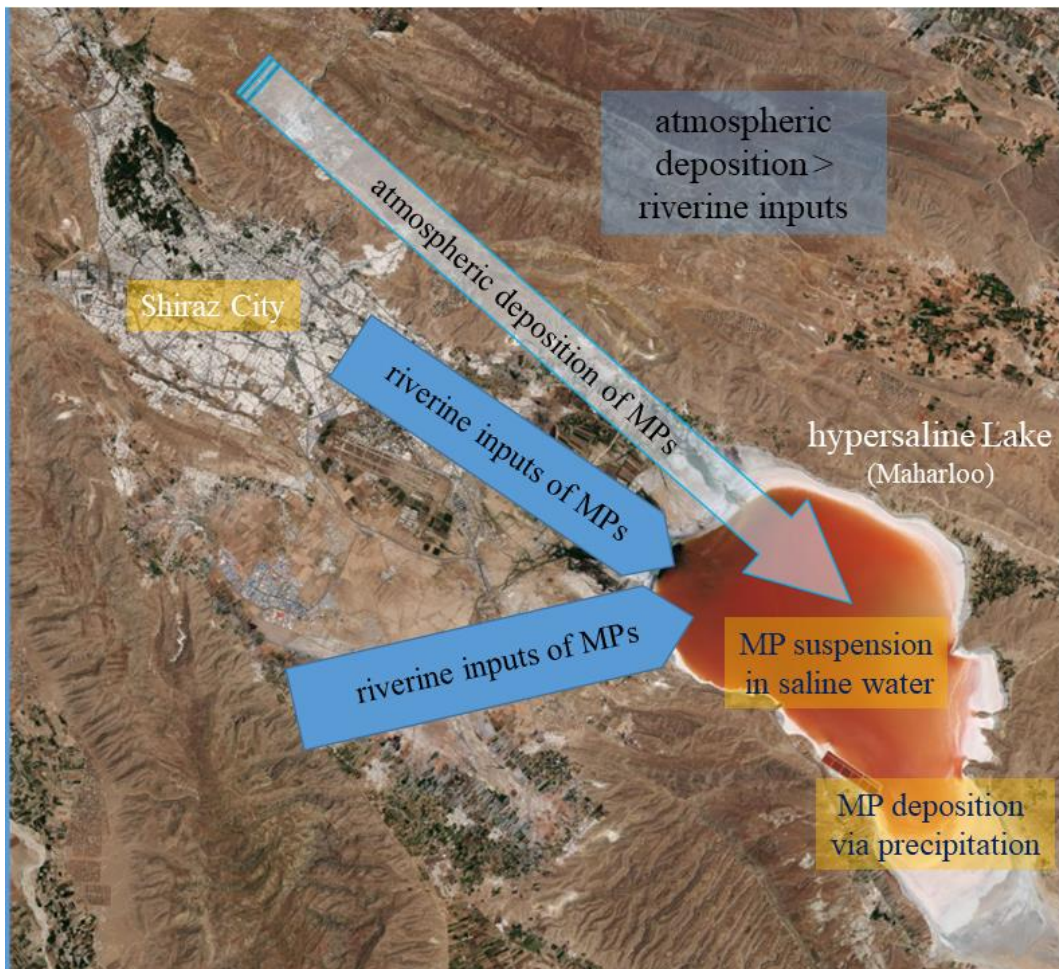
10
11 * Corresponding Author: Sajjad Abbasi; Department of Earth Sciences, College of Science, Shiraz
12 University, Shiraz 71454, Iran & Department of Radiochemistry and Environmental Chemistry,
13 Faculty of Chemistry, Maria Curie-Skłodowska University, Lublin 20-031, Poland

14 E-mail Address: sajjad.abbasi.h@gmail.com; sajjad.abbasi@shirazu.ac.ir

15
16 **Accepted 3 February 2022**

17 **<http://dx.doi.org/10.1016/j.scitotenv.2022.153721>**

33 Graphical Abstract



34

35

36

37

38 **Abstract**

39 Hypersaline lakes support unique ecosystems and biogeochemistries but are often subject to
40 anthropogenic pressures from pollution, water abstraction-diversion and climate change. Less
41 understood, however, are the inputs, distributions and impacts of microplastics (MPs) in hypersaline
42 environments. In this study, MPs are determined in water and sediment cores of Maharloo Lake,
43 south-west Iran, and in the anthropogenically-impacted rivers that recharge the lake. MP
44 concentrations in river water ranged from 0.05 MP L⁻¹ in the headwaters to about 2 MP L⁻¹
45 downstream of industrial effluents, with intermediate (but elevated) concentrations observed in the
46 lake. The maximum surface concentration in lake sediment cores was about 860 MP kg⁻¹, and
47 concentrations displayed a progressive reduction with increasing depth down to 50 cm that are
48 qualitatively consistent with temporal changes in plastic production. The size distribution of MPs was
49 skewed toward the finest fraction (< 100 µm) and the most abundant polymer types were
50 polyethylene terephthalate, polyethylene and nylon. Flux calculations using river water data and
51 published atmospheric deposition data for the region reveal that the atmosphere is, by at least an
52 order of magnitude, the more important source. MPs added to the lake appear to be maintained in
53 suspension by high density water but are subsequently deposited to sediments by encapsulation and
54 nucleation as salts precipitate. In addition, it is proposed that direct atmospheric deposition to
55 sediment takes place on areas that seasonally dry out and are subsequently inundated. The impacts
56 of MPs on hypersaline ecosystems and biomass resources are unknown but warrant investigation.

57

58 **Keywords:** rivers; sediments; polymers; brine; density; deposition

59

60

61 **1. Introduction**

62 Microplastics of < 5 mm in size are generated during the manufacture, usage and disposal of plastic
63 products and through the breakdown of plastic waste in the environment. Because of their low
64 density and slow degradation, MPs are ubiquitous and pervasive contaminants that have been
65 detected in regions far remote from any industrial or human use (Allen et al., 2019; Bergmann et al.,
66 2019; Abbasi et al., 2021).

67 An understanding of the transport, fluxes and impacts of MPs has relied on monitoring and empirical
68 studies in aquatic and terrestrial environments and in the atmosphere and an understanding of the
69 interplay between these different compartments (Allen et al., 2020; Liu et al., 2020). To this end,
70 surface aquatic systems appear to have received the most attention, and in particular oceans, rivers,
71 lakes, estuaries and the coastal zone (Rezania et al., 2018; Akdogan and Guven, 2019; Fu et al., 2020;
72 Manbohi et al. 2021). One type of aquatic system that has received very little study, however, is
73 coastal and inland hypersaline environments (Pashaei et al., 2021; Quesadas-Rojas et al., 2021).

74 Hypersaline lagoons and lakes represent a significant volume of inland water and are common in,
75 but not exclusive to, arid and semi-arid climates. Here, evaporation exceeds precipitation and salt
76 concentrations can approach or exceed saturation. In addition to high and variable salinities,
77 environmental stressors can include high levels of UV radiation, high temperatures and low oxygen
78 concentrations. Consequently, hypersaline environments host rather low microscopic and
79 macroscopic biodiversities (Naghoni et al., 2017). Despite these conditions, hypersaline systems
80 support important resources, such as salts for various industrial end-users and brine shrimp
81 (*Artemia*) cysts for aquaculture (Sorgeloos et al., 2001). Hypersaline environments also serve as
82 natural laboratories for studying the biology and biogeochemistry of evolution and adaptation and
83 for exploring novel approaches to biotechnology and bioremediation (Paul and Mormile, 2017).

84 Contaminated hypersaline lakes and lagoons also afford an opportunity to study the behaviour of
85 MPs under these unique conditions. For example, it is hypothesized that the high density of
86 hypersaline water allows a greater range of polymers to be suspended and dispersed, while
87 seasonal, evaporative loss of water means that hypersaline environments are predicted to be net
88 accumulators of MPs. In a recent study, Pashaei et al. (2021) determined the concentrations and
89 visible characteristics of MPs in a limited number of samples from Urmia Lake, north-west Iran, and
90 its tributary rivers, with one of the principal objectives centred around the testing of different
91 methods for MP detection. The authors found that the main source of MPs to the lake was from
92 rivers and that the lake itself acted as a sink of MPs through both physical and biological processes.
93 In the present study, and to improve our understanding of the sources, pathways and fates of MPs in

94 hypersaline environments, we conduct a more comprehensive investigation of the quantities and
95 characteristics of MPs in the water and sediment of a contaminated hypersaline lake in south-west
96 Iran (Maharloo Lake). Specifically, MPs sampled from lake water, tributary rivers impacted by urban
97 and industrial wastewaters and lake sediment cores are characterised by size, colour and polymer
98 type according to established techniques, and both riverine and atmospheric fluxes of MPs are
99 calculated from measurements in the tributaries and published depositional data for the region.

100

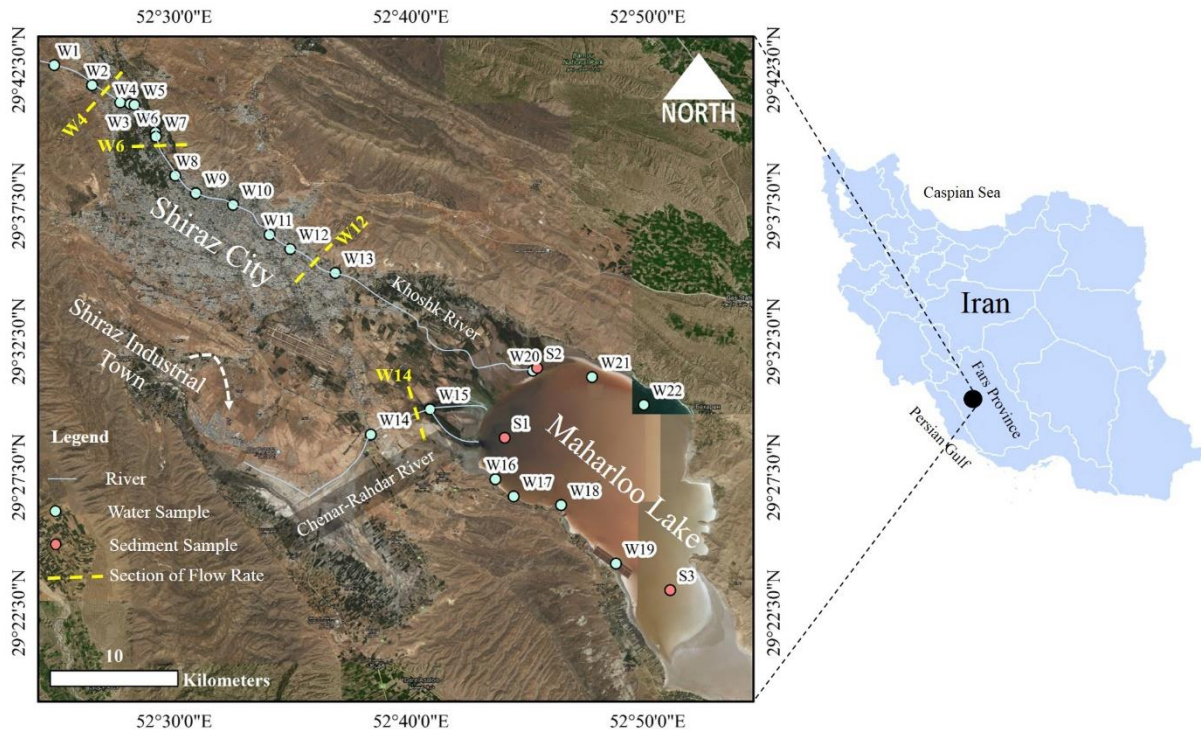
101 **2. Methods**

102 *2.1. Study site*

103 Maharloo Lake is a shallow, ephemeral saline lake covering an area of about 250 km² to the south-
104 east of the city of Shiraz and is one of the most important aquatic ecosystems in Iran (Sigaroodi et
105 al., 2014; Figure 1). The catchment area of the lake is about 4300 km² and has an average elevation
106 of about 1500 m. The region encompasses both arid and semi-arid climates and an annual rainfall
107 that ranges from 150 to 650 mm but that mainly falls between November and May (Amiri et al.,
108 2019). The bedrock of the lake is underlain by silty limestone and marl from the Oligo-Miocene age,
109 and the high salinity lake is due to the presence of Late Proterozoic salt domes in the catchment
110 (Forghani et al., 2012). Sediments consist of successive layers of halite, black, organic rich sediment,
111 green-grey sulphates, halite and carbonates, and fine, brown aluminosilicates, with the depths of
112 each layer exhibiting considerable spatial variation throughout the lake (Khosravi et al., 2020).

113 Maharloo Lake is recharged by direct precipitation on the surface, a series of springs along the
114 northern and western reaches, and two seasonal rivers: the Khoshk from the north-west and the
115 Chenar-Rahdar from the west. The Khoshk passes through the urbanised region of Shiraz and
116 receives direct inputs of treated and untreated sewage and industrial wastewater, while the Chenar-
117 Rahdar drains the industrial zone to the south of the city (established in 1992) and receives
118 considerable quantities of industrial wastes, including those from chemical and textile manufactures
119 (Moore et al., 2019). Over recent years, water supply to the lake has been declining because of
120 consecutive droughts, decreasing vegetative cover in the catchment and exploitation of water
121 resources by agriculture and industry (Daribi et al., 2021), and nowadays wastewater is often the
122 dominant input to the lake (Moore et al., 2019).

123



124
 125 Figure 1: Location of the sampling sites in Maharloo Lake and the Khoshk and Chenar-Rahdar Rivers.
 126 W = water, S = sediment; broken yellow lines denote locations where the water flow was measured.
 127

128 **2.2. Water sampling and processing**

129 A total of 22 sites were selected for sampling MPs from water (Figure 1). W1 and W2 were in the
 130 Khoshk River above the city of Shiraz and are considered as background sites in the catchment, W3
 131 to W13 were on the same river but within the urban area of the city, and W14 and W15 were on the
 132 Chenar-Rahdar River downstream of the industrial centre of Shiraz. W16 to W19 were located along
 133 the southern shores of Maharloo Lake and W20 to W22 were sampled from the northern shores. At
 134 four sites on the rivers (W4, W6, W12 and W14), current velocity was measured in the central
 135 channel using Valeport Model 001 rotating element current meter. Water flow at each site was
 136 calculated from the current velocity (in $m\ s^{-1}$) and estimated cross sectional area (in m^2).

137 Prior to sampling, all containers and equipment were washed with filtered tap water (0.45 μm
 138 Whatman Nylon membranes) and stored in aluminium foil, and during sampling, cotton clothing and
 139 nitrile gloves were worn by operators. The shallow, central channels of the rivers and the lake
 140 extending to about 1 km from the shoreline were accessed on foot in January 2021. Conductivity,
 141 temperature and pH were measured with a Eutech Instrument PCD 650 probe and floating and
 142 suspended MPs were collected from the top 25 cm of water in a 1-litre, wide-necked glass bottle.
 143 The contents of the bottle were subsequently passed through a 37 μm Nylon mesh net and the

144 procedure repeated until 20 L had been processed. With the aid of filtered water, material captured
145 by the net was transferred to a clean glass bottle as a suspension. In the laboratory, organic matter
146 was destroyed with a solution of filtered, saturated potassium hydroxide (Luo et al., 2019).
147 Specifically, a volume of KOH solution (KimiaExir) that was ten times the volume of the suspension
148 was added to the bottle, and the contents were covered with aluminium foil and left at room
149 temperature for 24 to 48 h before being filtered through a 1 µm-pore size Johnson cellulose test
150 membrane which was subsequently dried at room temperature in a covered glass Petri dish.

151

152 *2.3. Sediment sampling and processing*

153 Three sites were selected in Maharloo Lake for sediment core collection. S1 and S2 were located
154 near to the mouths of the Chenar-Rahdar River and the Khoskhk River, respectively, and where
155 riverine influence and sediment deposition are greatest. S3 was situated towards the southernmost
156 extremity of the lake in a region remote from any riverine inputs and where sediment deposition is
157 lowest. At each site, and within an area of about 4 m², five cores were taken manually using a
158 custom-made, 5 cm diameter, 50 cm stainless steel corer. On site, cores were dissected using a
159 stainless steel spatula into five depths (0-10 cm, 10-20 cm, 20-30 cm, 30-40 cm and 40-50 cm) and
160 sediment from each depth was combined to provide a series of composites.

161 In the laboratory, sediment samples ($n = 15$) were homogenised using a glass spatula, dried at room
162 temperature in a clean room and sieved through a 5-mm stainless steel sieve before MPs were
163 isolated according to Abbasi et al. (2021). Thus, 100 g of each sample were digested with 100 mL of
164 35% H₂O₂ (Arman Sina) for 7 d in a series of 150 mL glass beakers covered with aluminium foil. The
165 remaining contents were vacuum-filtered through 2 µm S&S filter paper (blue band, grade 589/3),
166 washed with filtered tap water and dried in a sand bath at 60 °C in clean beakers. Seventy mL of
167 ZnCl₂ solution (KimiaExir; density ~ 1.6 to 1.8 g cm⁻³) was added to each sample before the contents
168 were agitated for 5 min at 350 rpm and subsequently allowed to settle for 90 min. The remaining
169 solution was decanted, centrifuged for 3 min at 4000 rpm and vacuum filtered through 2 µm.
170 Density separation, centrifugation and filtration was then repeated twice more. No background
171 contamination was found by replicating the procedure in the absence of sediment.

172

173 *2.4. Identification and characterisation of microplastics*

174 MPs retained on filters arising from the processing of water and sediment samples were identified,
175 counted and characterised under a binocular microscope (Carl-Zeiss, Köln, Germany) at up to 200-x

176 magnification with the aid of a 250 μm -diameter stainless steel probe and ImageJ software (Abbasi
177 and Turner, 2021). MP identification was based on visible characteristics (shininess, thickness,
178 hardness, surface and cross sectional structures) and reaction to the heated probe according to
179 protocols outlined elsewhere (Abbasi et al., 2019). Classification was based on shape (fibre, film,
180 fragment or spherule), length of the longest axis, L ($L < 100 \mu\text{m}$, $100 \leq L < 250 \mu\text{m}$, $250 \leq L < 500 \mu\text{m}$,
181 $500 \leq L < 1000 \mu\text{m}$, $L \geq 1000 \mu\text{m}$; and with a size detection limit of 30 to 50 μm depending on
182 shape), and colour (black-grey, yellow-orange, white-transparent, red-pink or blue-green).

183 The polymeric makeup of 48 MPs of a range of shapes, sizes and colours and isolated from water (n
184 = 24) and sediment ($n = 24$) from different locations was determined using a micro-Raman
185 spectrometer (μ -Raman-532-Ci, Avantes, Apeldoorn, Netherland) with a laser of 785 nm and Raman
186 shift of 400-1800 cm^{-1} .

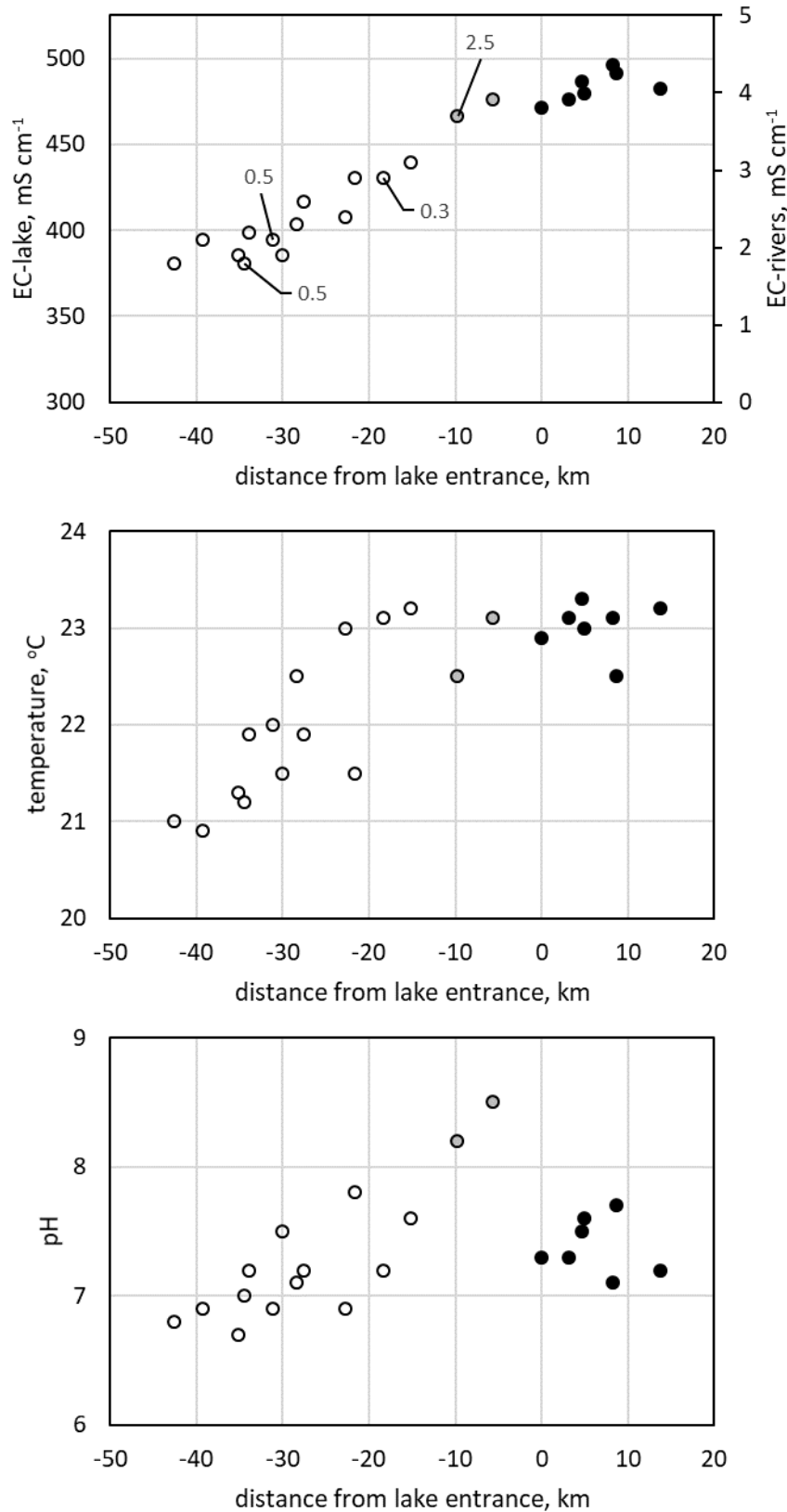
187

188 **3. Results**

189 *3.1. Water characteristics and river discharge*

190 The physico-chemical characteristics of the water samples are shown in Figure 2 as a function of
191 distance from the entrance of the River Khoshk or River Chenar-Rahdar to Maharloo Lake. Electrical
192 conductivity (EC), as specific conductance, exhibits a clear downstream increase in the rivers from
193 about 1.8 mS cm^{-1} in the upper reaches of the Khoshk River to about 4 mS cm^{-1} near to the mouth of
194 the Chenar-Rahdar River, and is two orders of magnitude greater in the lake (averaging about 480
195 mS cm^{-1}). Temperature exhibits an increase of about 2°C from the upper Khoshk River to Maharloo
196 Lake while the distribution of pH is more variable and the highest values are in the lower Chenar-
197 Rahdar River.

198 Also shown in Figure 2 are the four estimates of water flow in the rivers. For the Khoshk River,
199 estimates are 0.5 $\text{m}^3 \text{s}^{-1}$ in the upper catchment and decline to 0.3 $\text{m}^3 \text{s}^{-1}$ in the city of Shiraz, while in
200 the Chenar-Rahdar River, the single estimate is 2.5 $\text{m}^3 \text{s}^{-1}$. According to the Fars Regional Water
201 Authority data, the monthly average flows for January recorded between 1988 and 2015 in the
202 upper and lower Khoshk River and in the Chenar-Rahdar River are 1.9, 1.4 and 4.3 $\text{m}^3 \text{s}^{-1}$,
203 respectively, with minima and maxima of 0.1, < 0.1 and 0.5 $\text{m}^3 \text{s}^{-1}$ and 4.6, 8.2 and 22.8 $\text{m}^3 \text{s}^{-1}$,
204 respectively.



205

206 **Figure 2:** Electrical conductivity (EC), temperature and pH of the water samples from which MPs
 207 were isolated. Data are shown as a function of axial distance upstream (negative values: Khoshk
 208 River, open circles; river Chenar-Rahdar River, grey circles) and direct distance downstream (positive

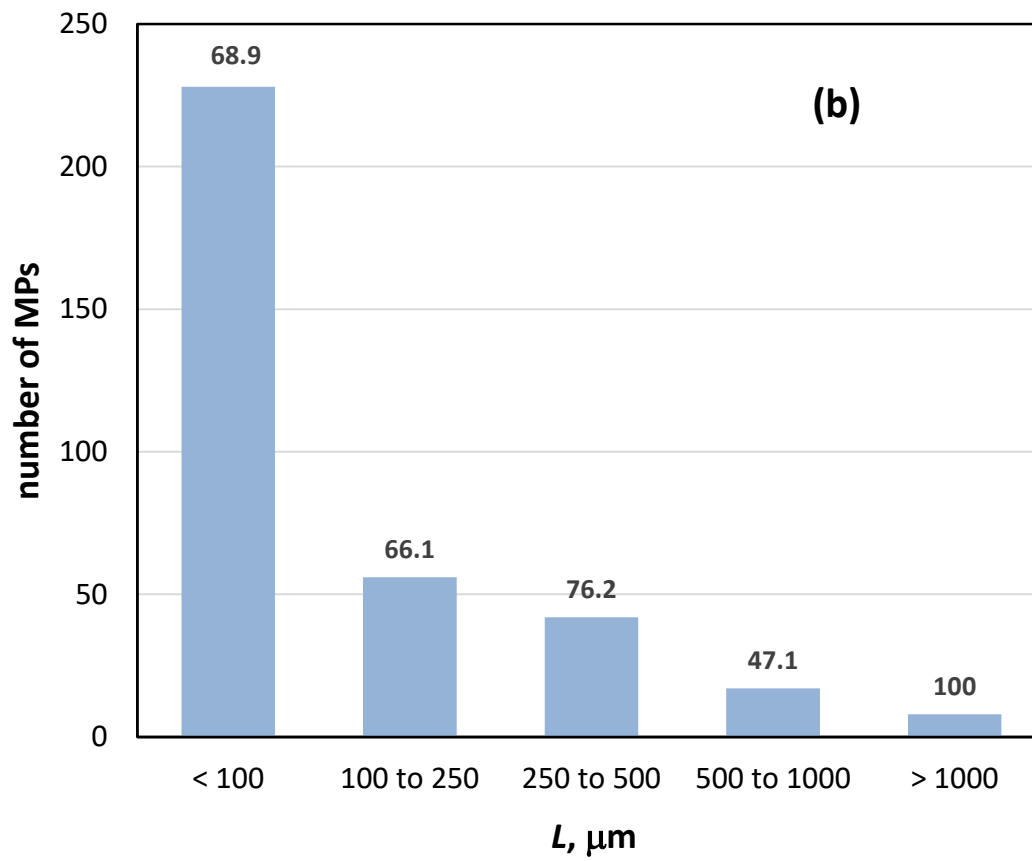
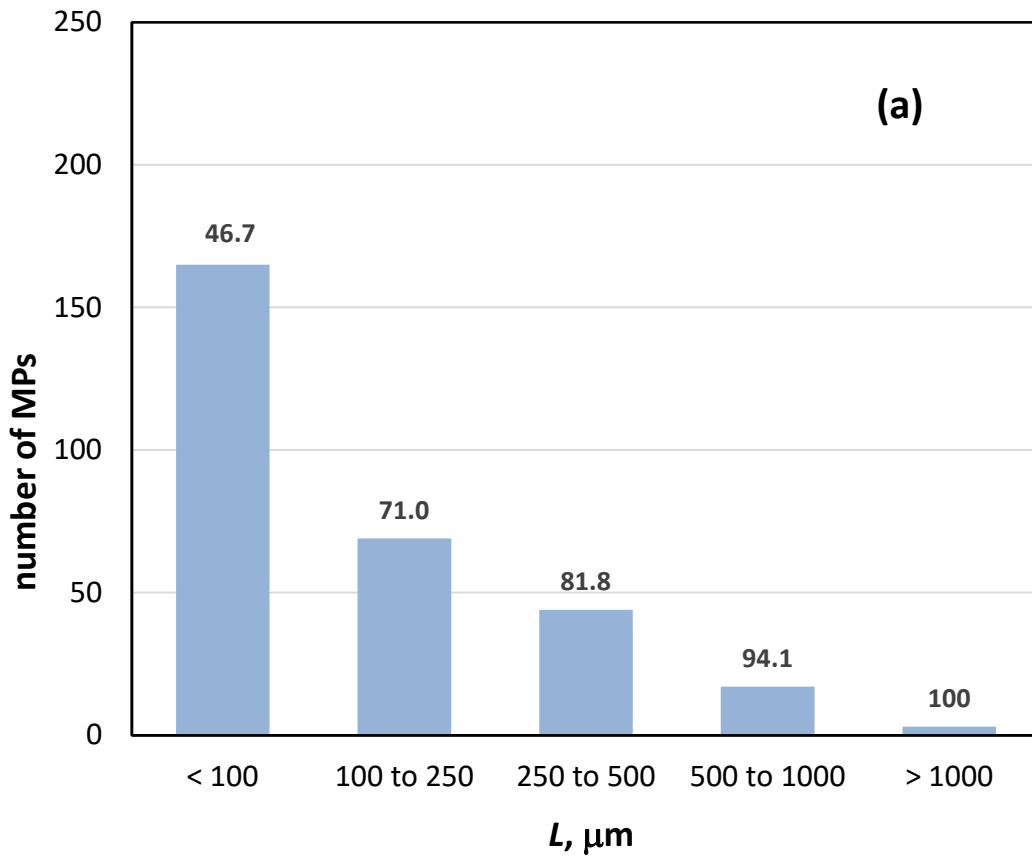
209 values: Maharloo Lake, black circles) from the lake entrance, with the latter defined as the mouth of
210 the corresponding river and where downstream distance in the lake is measured from the nearest
211 river mouth. Note the change of scale for EC from river water to lake water. Annotated on the EC-
212 distance chart are estimates of water flow in $\text{m}^3 \text{s}^{-1}$.

213

214 *3.2. Microplastics in water samples*

215 Overall, 298 MPs were isolated from the 22 water samples, and of these 181 (or 60.7%) were fibres
216 that were roughly equally distributed amongst the different colour categories. Spherules totalled 65
217 (or 21.8%) of MPs, and all but three detected were black-grey in colour. Films and fragments
218 represented 11.4% and 6.0% of MPs and all colour categories were represented by both shape
219 types. The distribution of MP as a function of size, illustrated in Figure 3a, reveals a declining number
220 with increasing length category. However, and as annotated in the figure, the proportion of fibrous
221 MPs increases with increasing length.

222



224 Figure 3: Overall size distribution of MPs isolated from (a) water samples in the Khoshk and Chenar-
225 Rahdar Rivers and Maharloo Lake and (b) sediment samples from Maharloo Lake. Numbers
226 annotated are the percentages of fibres in each size category.

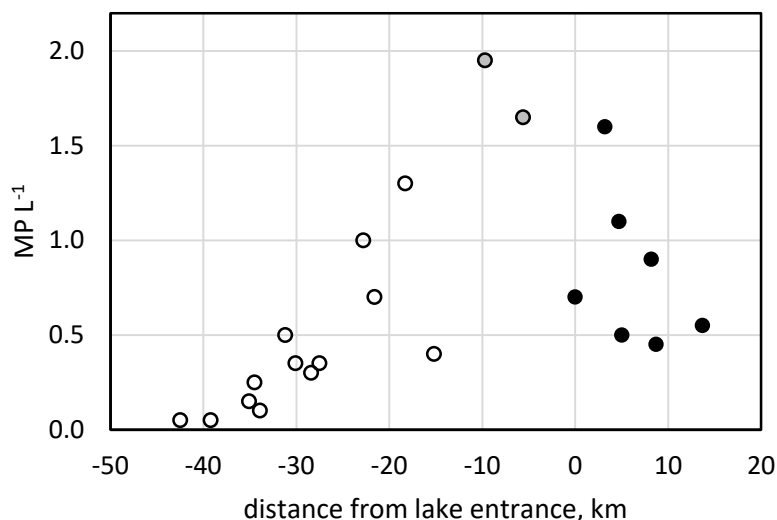
227

228 Figure 4 shows the distribution of MP concentrations in surface waters of the rivers and lake as a
229 function of distance from Maharloo Lake entrance. In the Khoshk River, concentrations exhibit a
230 progressive increase from 0.05 MP L⁻¹ in the reaches above the influence of the city of Shiraz (W1
231 and W2) to about 1.3 MP L⁻¹ at site W12 within the urban district. The concentration thereafter
232 declines as the river leaves Shiraz and nears the lake entrance. The highest MP concentrations were
233 found at the two sites in the Chenar-Rahdar River, and concentrations in the lake were between the
234 lowest and highest riverine concentrations (but always greater than nine river samples) and
235 exhibited a broad reduction with increasing distance from the riverine inputs.

236

237 3.3. Microplastics in sediment cores

238 Regarding the sediment cores, 351 MPs were retrieved and 242 (68.9%) were fibres, of which about
239 60% were black-grey or white-transparent. Films and fragments of various colours represented 8.5%
240 and 17.7% of MPs but spherules comprised only 4.8%. Consistent with MPs in the water samples,
241 and illustrated in Figure 3b, the size distribution of sediment MPs exhibits a reduction in number
242 (albeit more pronounced) and an overall increase in the proportion of fibres with increasing length.
243 The vertical distributions of MPs in the three sediment cores (with each derived from combining five
244 individual cores) are shown in Figure 5. There is a decline in MP number with increasing sediment
245 depth in all cores, and MPs below 100 µm in length make the largest contribution to the MP pool in
246 each case; note also the absence of MPs in larger size categories in the deepest section of each core.



247

248 Figure 4: Concentration of MPs per L of water in as a function of axial distance upstream (Khoshk
 249 River, open circles; river Chenar-RahdarRiver, grey circles) and direct distance downstream
 250 (Maharloo Lake, black circles) from the lake entrance, with the latter defined as the mouth of the
 251 corresponding river and where downstream distance in the lake is measured from the nearest river
 252 mouth.

253

254 3.4. Microplastics by polymer type

255 The results of the μ -Raman analysis of MPs retrieved from the water samples and sediment cores
 256 are presented in Table 1. The same six polymer types (whose densities are also indicated) were
 257 detected in both sets of MPs, with polyvinyl chloride (PVC) notably more abundant in the sediment
 258 than suspended in the water and nylon most abundant overall. With the exception of polyethylene,
 259 all polymer types were detected in both fibrous and non-fibrous MPs.

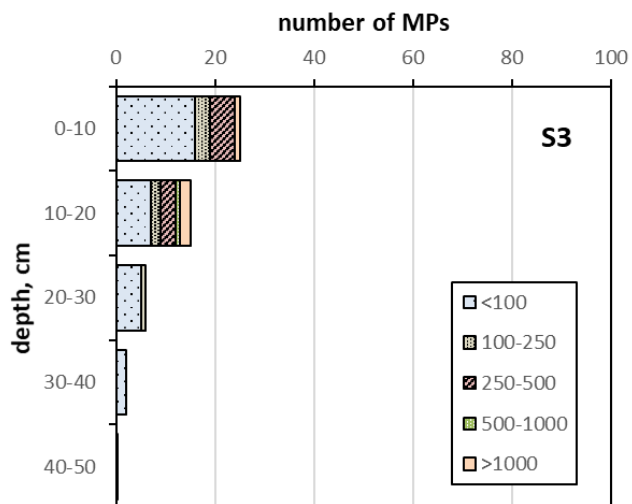
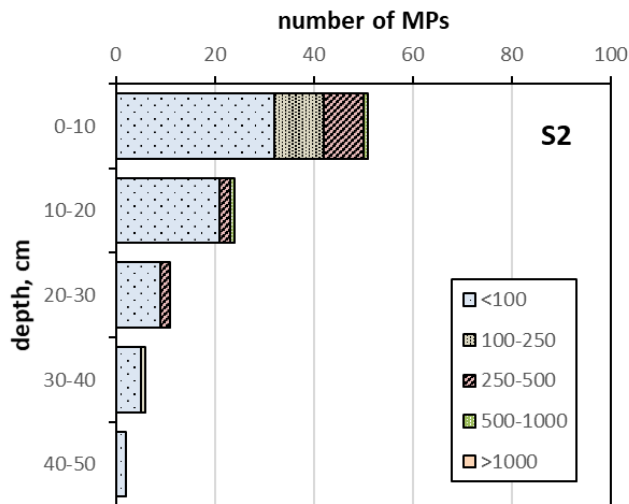
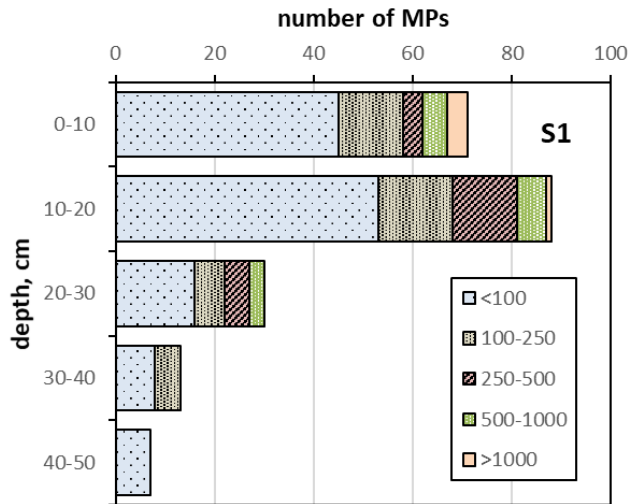
260

261 Table 1: Distribution of MPs retrieved from water and sediment samples (that were analysed by μ -
 262 Raman spectroscopy) by polymer type and shown in order of decreasing polymer density.

polymer	density, g cm ⁻³	water		sediment	
		total	fibres	total	fibres
polyvinyl chloride	1.38	1	0	4	3
polyethylene terephthalate	1.38	4	4	6	5
nylon	1.15	8	6	5	4
polystyrene	1.05	4	4	3	2
polyethylene	0.86 to 0.98	5	5	5	5
polypropylene	0.89 to 0.92	2	1	1	1

263

264



265

266 Figure 5: Number and size distribution (in μm) of MPs in combined 100-g sediment samples as a
 267 function of core depth.

268 4. Discussion

269 The results of the study reveal that industrial and urban inputs dramatically increase the
270 concentrations of MPs in river water. Specifically, a background concentration of 0.05 MP L^{-1} in the
271 headwaters that most likely reflects atmospheric deposition and inputs from agricultural practices in
272 the catchment is augmented up to about 2 MP L^{-1} downstream of anthropogenic inputs by MPs of a
273 greater diversity of shapes and sizes. The concentrations of MPs on a number basis in other rivers
274 reported in the literature are highly variable, being dependent on factors like climate, hydrology,
275 land use, anthropogenic activities, sampling design and means of MP identification (Kapp and
276 Yeatman, 2018; Mani and Burkhardt-Holm, 2020; Zhang et al., 2021). Nevertheless, the highest
277 concentration determined in the present study is close to the maximum concentrations reported for
278 a number of urbanised rivers in China (4 to 7.2 MP L^{-1} ; Luo et al., 2019) and an urbanised river in
279 Portugal (1.3 MP L^{-1} ; Rodrigues et al., 2018), and to the median concentration reported for various
280 polluted Dutch rivers (0.86 MP L^{-1} ; Mintenig et al., 2020). That MP concentrations throughout
281 Maharloo Lake are higher than concentrations in seven river samples impacted by wastewater
282 inputs requires additional, non-riverine sources of MP to the lake and/or mechanisms by which MPs
283 accumulate and evade ready removal from the water column.

284 The concentrations of MPs and water discharge rates measured towards the mouths of the Khoshk
285 and Chenar-Rahdar Rivers (see Figures 2a and 4) yield respective riverine fluxes into the lake of
286 about 400 and 5000 MP s^{-1} , or about 3×10^7 and $4 \times 10^8 \text{ MP}$ per day. Extrapolating to an annual basis
287 is more uncertain because of significant seasonal variations in river flow and, likely, MP inputs from
288 urban and industrial sources. Nevertheless, using the long-term mean monthly discharges of the
289 Khoshk and Chenar-Rahdar Rivers of 0.84 and $2.1 \text{ m}^3 \text{ s}^{-1}$ and the MP concentrations determined
290 herein results in MP flux estimates of 3.4×10^{10} and 1.3×10^{11} , respectively, or a total annual riverine
291 input of MPs about 1.6×10^{11} .

292 For comparative purposes, the daily and annual fluxes of MPs to Lake Maharloo from the
293 atmosphere can be estimated from monthly dry and wet depositional data reported for both the city
294 of Shiraz and Mount Derak, a remote area 20 km to the north west of Shiraz, by Abbasi and Turner
295 (2021). Specifically, data for Shiraz are representative of conditions when wind carries air from the
296 city to the south east, while data for Mount Derak are more representative of calmer conditions or
297 when winds are from a more southerly direction. Shiraz data for January indicate a total (dry and
298 wet) deposition of MPs of about 1000 per m^{-2} , resulting in a deposition of about 2.5×10^{11} for the
299 average area of Lake Maharloo (250 km^2), and a daily deposition of about $8.3 \times 10^9 \text{ MP}$ at this time of
300 year. The annual deposition of MPs from the atmosphere at Shiraz is about 24000 per m^{-2} , yielding a

301 total deposition over the average lake area of about 6.0×10^{12} per annum. Mount Derak data for
302 January indicate a total deposition of about 230 MP per m^{-2} , yielding monthly and daily deposition
303 rates of about 5.7×10^{10} and 1.9×10^9 , respectively, for Lake Maharloo. The annual deposition of
304 MPs over Mount Derak is about 5000 MP m^{-2} , resulting in a total annual deposition of MPs of about
305 1.3×10^{12} . It is likely, therefore, that the atmospheric flux to Lake Maharloo is somewhere between
306 these estimates, but with dominant north-westerly winds suggesting a value closer to that derived
307 from Shiraz data. Nevertheless, both estimates indicate an atmospheric flux that is at least an order
308 of magnitude greater than the riverine flux and which can at least partly explain the apparent
309 enrichment of MPs in the lake waters relative to the inflowing rivers.

310 The fate of MPs derived from the rivers and atmosphere, or any other sources around the lake itself
311 (e.g. tourism, recreation, agriculture and traffic), will be determined to a large extent by buoyancy.
312 To this end, therefore, the density of Maharloo Lake water itself is a critical factor. The specific
313 conductance of the lake samples averages about 480 mS cm^{-1} , and this is equivalent to a salinity of
314 about 385 parts per thousand. Assuming that halite is the principal salt present in the lake (Khosravi
315 et al., 2020), the water is saturated with a density of about 1.2 g cm^{-3} (Sigma-Aldrich, 2018). Such a
316 high density inhibits the settlement of four out of six polymer types detected, or, according to Table
317 1, about 80% of the MPs in lake water. This also accounts for the abundance of MPs in the waters of
318 Maharloo Lake, as well as the diversity of polymers observed. By comparison, a recent global review
319 of MPs in lakes undertaken by Dusaucy et al. (2021) revealed that, overall, the dominant polymers
320 were polyethylene and polypropylene, whose presence was attributed to global demand but would
321 also be anticipated based on buoyancy considerations in fresh water.

322 In an environment as saline as Maharloo Lake, the accumulation of a range of MP types (and
323 densities) in the sediment requires mechanisms other than inherent settlement through the water
324 column. Aggregation with denser particulates or packaging in faecal matter of plastic-ingesting
325 organisms such as the brine shrimp (*Artemia parthenogenetica*) may accelerate the settlement and
326 deposition of some MPs (Hafezieh, 2003; Pashaei et al., 2021). However, the more general
327 deposition is likely to proceed via the nucleation of and the encapsulation with salts that are super-
328 saturated in the lake, and in particular during late summer when insolation is high and rainfall low
329 (Pashaei et al., 2021). Inundation of salt deposits in wetter months may subsequently lead to the
330 partial release of MPs back into the water column, while remaining MPs and salts become trapped in
331 the sediment layer by depositing particulate matter. In addition to these processes, MP
332 accumulation on sediment and salt crystals exposed in the dry months may also take place more
333 directly via atmospheric deposition.

334 The decrease in MP concentrations in the sediment cores from locations S1 to S3 is likely due to the
335 increasing distance from both the mouths of the tributaries (as a riverine source) and the city of
336 Shiraz (as an atmospheric source), while the decline in MP concentrations with increasing sediment
337 depth in each core reflects temporal changes in the supply of MPs. Estimates based on ¹³⁷Cs
338 activities in Maharloo Lake sediment suggest average depositional rates of about 1 cm per year
339 (Mesbah and Amidi, 2006) and that our 50 cm cores, therefore, encompass a 50-year period of
340 deposition. Within this timeframe, there has been a general, exponential increase in the production
341 and environmental emission of plastics (Geyer et al., 2017), and since 1992 there has been an
342 increase in MP fluxes to the lake associated with the construction of the industrial centre to the
343 south of Shiraz. Similar distributions of MPs in sediment cores from many temperate and subtropical
344 (but not seasonal) urban lakes and estuaries have been attributed to increasing plastic use and
345 disposal over the past few decades (Willis et al., 2017; Fan et al., 2019; Turner et al., 2019). An
346 additional factor that may accentuate the vertical reduction in MP concentrations in Maharloo Lake
347 sediment cores is a gradual decline in the delivery of water and sediment to the lake that act to
348 dilute MPs in both river water and depositing particulate matter.

349 More generally, the present study suggests that, through riverine and atmospheric inputs and
350 seasonal, evaporative loss of surface water, hypersaline lakes are likely to act as accumulators of
351 MPs. Moreover, the high density of these lake waters is able to disperse and deposit a wider range
352 of polymer types than freshwater lentic environments. To this end, sediment cores in hypersaline
353 lakes could provide a more representative, historical record of plastic uses and their inputs to the
354 environment and any relationships with shifting climate than those obtained in other settings. The
355 accumulation of a broad range of MPs in hypersaline lakes may also present specific threats to
356 halophilic ecosystems, including those used to understand fundamental biological concepts and
357 improve various biotechnologies, and to economic and non-economic resources (e.g., minerals,
358 biomass and wading birds) (Gündoğdu, 2018; Pashaei et al., 2021).

359

360 **Acknowledgments**

361 We thank Shiraz University (Grant No. 99GRC1M371631) for financially supporting the project, and
362 Ali Abbasi for assistance with sampling.

363

364

365 **References**

- 366 Abbasi, S., Turner, A., 2021. Dry and wet deposition of microplastics in a semi-arid region (Shiraz,
367 Iran). *Science of the Total Environment* 786, 147358.
- 368 Abbasi, S., Keshavarzi, B., Moore, F., Turner, A., Kelly, F.J., Dominguez, A.O., Jaafarzadeh, N., 2019.
369 Distribution and potential health impacts of microplastics and microrubbers in air and street dusts
370 from Asaluyeh County, Iran. *Environmental Pollution* 244, 153–164.
- 371 Abbasi, S., Turner, A., Hoseini, M., Amiri, H., 2021. Microplastics in the Lut and Kavir Deserts, Iran.
372 *Environmental Science and Technology* 55, 5993-6000.
- 373 Akdogan, Z., Guven, B., Microplastics in the environment: A critical review of current understanding
374 and identification of future research needs. *Environmental Pollution* 254, 113011.
- 375 Allen, S., Allen, D., Phoenix, V.R., Le Roux, G., Jimenez, P.D., Simonneau, A., Binet, S., Galop, D., 2019.
376 Atmospheric transport and deposition of microplastics in a remote mountain catchment. *Nature*
377 *Geoscience* 12, 339-344.
- 378 Allen, S., Allen, D., Moss, K., Le Roux, G., Phoenix, V.R., Sonke, J.E., 2020. Examination of the ocean as
379 a source for atmospheric microplastics. *PLoS ONE* 15, e0232746.
- 380 Amiri, M., Pourghasemi, H.R., Ghanbarian, G.A., Afzali, S.F., 2019. Assessment of the importance of
381 gully erosion effective factors using Boruta algorithm and its spatial modeling and mapping using
382 three machine learning algorithms. *Geoderma* 340, 55-69.
- 383 Bergmann, M.; Mützel, S.; Primpke, S.; Tekman, M.B.; Trachsel, J.; Gerdts, G. White and wonderful?
384 Microplastics prevail in snow from the Alps to the Arctic. *Sci. Adv.* 2019, 5, eaax1157.
- 385 Darabi, H., Moradi, E., Davudirad, A.A., Ehteram, M., Cerda, A., Haghghi, A.T., 2021. Efficient
386 rainwater harvesting planning using socio-environmental variables and data-driven geospatial
387 techniques. *Journal of Cleaner Production* 311, 127706.
- 388 Dusaucy, J., Gateuille, D., Perrette, Y., Naffrechoux, E., 2021. Microplastic pollution of worldwide
389 lakes. *Environmental Pollution* 284, 117075.
- 390 Fan, Y.J., Zheng, K., Zhu, Z.W., Chen, G.S., Peng, X.Z., 2019. Distribution, sedimentary record, and
391 persistence of microplastics in the Pearl River catchment, China. *Environmental Pollution* 251, 862-
392 870.
- 393 Forghani, G., Moore, F., Lee, S., Qishlaqi, A., 2009. Geochemistry and speciation of metals in
394 sediments of the Maharlu Saline Lake, Shiraz, SW Iran. *Environmental Earth Sciences* 59, 173-184.
- 395 Fu, Z.L., Chen, G.L., Wang, W.J., Wang, J., 2020. Microplastic pollution research methodologies,
396 abundance, characteristics and risk assessments for aquatic biota in China. *Environmental Pollution*
397 266, 115098.
- 398 Geyer, R., Jambeck, J.R., Law, K.L., 2017. Production, use, and fate of all plastics ever made. *Scientific*
399 *Advances* 3, e1700782.
- 400 Gündoğdu, S., 2018. Contamination of table salts from Turkey with microplastics. *Food Additives &*
401 *Contaminants: Part A* 35, 1006-1014.
- 402 Hafezieh, M., 2003. Some biological aspects and biomass estimation of *Artemia* in Maharloo Lake.
403 *Iranian Scientific Fisheries Journal* 11, 11-28.

404 Kapp, K.J., Yeatman, E., 2018. Microplastic hotspots in the Snake and Lower Columbia rivers: A
405 journey from the Greater Yellowstone Ecosystem to the Pacific Ocean. *Environmental Pollution* 241,
406 1082-1090.

407 Khosravi, R., Zarei, M., Sracek, O., 2020. Hydraulic and geochemical interactions between surface
408 water and sediment pore water in seasonal hypersaline Maharlu Lake, Iran. *Hydrological Processes*
409 34, 3358-3369.

410 Liu, K., Wang, X., Song, Z., Wei, N., Haoda, Y., Cong, X., Zhao, L., Li, Y., Qu, L., Zhu, L., Zhang, F., Zong,
411 C., Jiang, C., Li, D., 2020. Global inventory of atmospheric fibrous microplastics input into the ocean:
412 An implication from the indoor origin. *Journal of Hazardous Materials* 400, 123223.

413 Luo, W., Su, L., Craig, N.J., Du, F., Wu, C., Shi, H., 2019. Comparison of microplastic pollution in
414 different water bodies from urban creeks to coastal waters. *Environmental Pollution* 246, 174-182.

415 Manbohi, A., Mehdiinia, A., Rahnama, R., Dehbandi, R., 2021. Microplastic pollution in inshore and
416 offshore surface waters of the southern Caspian Sea. *Chemosphere* 281, 130896.

417 Mani, T., Burkhardt-Holm, P., 2020. Seasonal microplastics variation in nival and pluvial stretches of
418 the Rhine River - From the Swiss catchment towards the North Sea. *Science of the Total Environment*
419 707, 135579.

420 Mesbah, S.H., Amidi, J., 2006. Annual sedimentation rate of Maharloo Lake using ¹³⁷Cs (in Persian).
421 Persian National Conference on Sediment, Iranian Watershed Management Association.

422 Mintenig, S.M., Kooi, M., Erich, M.W., Primpke, S., Redondo-Hasselerharm, P.E., Dekker, S.C.,
423 Koelmans, A.A., van Wezel, A.P., 2020. A systems approach to understand microplastic occurrence
424 and variability in Dutch riverine surface waters. *Water Research* 176, 115723.

425 Moore, F., Birami, F.A., Keshavazri, B., Kamali, M., 2019. Potentially toxic elements contamination in
426 sediment, surface and pore water of Maharlu Saline Lake, South – West Iran. *Geopersia* 9, 111-124.

427 Naghoni, A., Emtiazi, G., Amoozegar, M.A., Cretoiu, S., Stal, L.J., Etemadifar, Z., Abolhassan, S., Fazeli,
428 S., Bolhuis, H., 2017. Microbial diversity in the hypersaline Lake Meyghan, Iran. *Scientific Reports* 7,
429 11522.

430 Pashaei, R., Loiselle, S.A., Leone, G., Tamasi, G., Dzingelevič, R., Kowalkowski, T., Gholizadeh, M.,
431 Consumi, M., Abbasi, S., Sabaliauskaite, V., Buszewski, B., 2021. Determination of nano and
432 microplastic particles in hypersaline lakes by multiple methods. *Environmental Monitoring and*
433 *Assessment* 193, 668.

434 Paul, V.G., Mormile, M.R., 2017. A case for the production of saline and hypersaline environments: A
435 microbiological perspective. *FEMS Microbiology Ecology* 93, fix091. doi: 10.1093/femsec/fix091

436 Quesadas-Rojas, M., Enriquez, C., Valle-Levinson, A., 2021. Natural and anthropogenic effects on
437 microplastic distribution in a hypersaline lagoon. *Science of the Total Environment* 776, 145803.

438 Rezania, S., Park, J., Din, M.F.M., Taib, S.M., Talaiekhosani, A., Yadav, K.K., Kamyab, H., 2018.
439 Microplastics pollution in different aquatic environments and biota: A review of recent studies.
440 *Marine Pollution Bulletin* 133, 191-208.

441 Rodrigues, M.O., Abrantes, N., Gonçalves, F.J.M., Nogueira, H., Marques, J.C., Gonçalves, A.M.M.,
442 2018. Spatial and temporal distribution of microplastics in water and sediments of a freshwater

443 system (Antuã River, Portugal). *Science of the Total Environment* 633, 1549-1559.
444

445 Sigaroodi, S.K., Chen, Q., Ebrhimi, S., Nazari, A., Choobin, B., 2014. Long-term precipitation forecast
446 for drought relief using atmospheric circulation factors: a study on the Maharloo Basin in Iran.
447 *Hydrological Earth Systems Science* 18, 1995-2006.

448 Sigma-Aldrich, 2018. 71376, 71386 Sodium chloride (halite, common salt or table salt, rock salt).
449 [https://www.sigmaaldrich.com/deepweb/assets/sigmaaldrich/product/documents/179/430/71386d](https://www.sigmaaldrich.com/deepweb/assets/sigmaaldrich/product/documents/179/430/71386dat.pdf)
450 [at.pdf](https://www.sigmaaldrich.com/deepweb/assets/sigmaaldrich/product/documents/179/430/71386dat.pdf) accessed 11/21.

451 Sorgeloos, P., Dhert, P., Candreva, P., 2001. Use of the brine shrimp, *Artemia* spp., in marine fish
452 larviculture. *Aquaculture* 200, 147-159.

453 Turner, S., Horton, A.A., Rose, N.L., Hall, C., 2019. A temporal sediment record of microplastics in an
454 urban lake, London, UK. *Journal of Paleolimnology* 61, 449-462.

455 Xu, Y., Chan, F.K.S., Johnson, M., Stanton, T., He, J., Jia, T., Wang, J., Wang, Z., Yao, Y., Yang, J., Liu, D.,
456 Xu, Y., Yu, X., 2021. Microplastic pollution in Chinese urban rivers: The influence of urban factors.
457 *Recycling* 173, 105686.

458 Willis, K.A., Eriksen, R., Wilcox, C., Hardesty, B.D., 2017. Microplastic distribution at different
459 sediment depths in an urban estuary. *Frontiers in Marine Science* 4, 419.

460

461 Zhang, Z.Q., Deng, C.N., Dong, L., Liu, L.S., Li, H.S., Wu, J., Ye, C.L., 2021. Microplastic pollution in the
462 Yangtze River Basin: Heterogeneity of abundances and characteristics in different environments.
463 *Environmental Pollution* 287, 117580.

464

465